Bark cloth structure and properties: A naturally occurring fabric and ancestral textile craft from Uganda

Emmanuelle Richely, Darshil Shah, Sylvie Durand, Victor Gager, Camille Goudenhooft, Delphin Pantaloni, Dieuveil Ngoubou, Catherine Lapierre, Sylvie Chevallier, Hom Dhakal, et al.

Industrial Crops & Products 215 (2024) 118613

Contents lists available at ScienceDirect

Industrial Crops & Products

journal homepage: www.elsevier.com/locate/indcrop

Bark cloth structure and properties: A naturally occurring fabric and ancestral textile craft from Uganda

Emmanuelle Richely [a], Darshil Shah [b], Sylvie Durand [a], Victor Gager [c], Camille Goudenhooft [c], Delphin Pantaloni [c], Dieuveil Ngoubou [d], Sylvie Chevallier [e], Hom Dhakal [f], Sofiane Guessasma [a], Richard Sibout [a], Catherine Lapierre [g], David Legland [a], Guilhem Blès [h], Johnny Beaugrand [a], Alain Bourmaud [c,*]

[a] INRAE, UR1268 BIA Biopolymères Interactions Assemblages, Nantes, France
[b] Centre for Natural Material Innovation, Department of Architecture, University of Cambridge, Cambridge, UK
[c] Univ. Bretagne Sud, UMR CNRS 6027, IRDL, Lorient F-56100, France
[d] UMOJA COMPANY FAIRTRADE, 2 Rue François Verny, Brest 29200, France
[e] UMR GEPEA CNRS 6144 - ONIRIS, Nantes Cedex 3 44322, France
[f] Advanced Polymers and Composites (APC) Research Group, School of Mechanical and Design Engineering, University of Portsmouth, Hampshire PO1 3DJ, UK
[g] INRAE, AgroParisTech, Université Paris Saclay, IJPB, Versailles, France
[h] ENSTA Bretagne, UMR CNRS 6027, IRDL, Brest, France

ARTICLE INFO

Keywords:
Plant fibres
Biochemical properties
Crystallinity
Mechanical properties
Computing

ABSTRACT

Natural fabrics from two bark trees of Uganda ("Kilundu": *Antiaris toxicaria* and "Mutuba": *Ficus natalensis*) are being considered today for the local footwear industry. Here, we thoroughly examined to determine their structural, biochemical and mechanical properties of the two bark cloths, in order to ascertain their potential use as locally-available, low-cost composite reinforcements and eventually for a use in textile industry as well. Fibres in both fabrics are rich in highly crystalline cellulose (76.6 ± 4.9% and 66.3 ± 0.5%) and have very cohesive cell walls with small lumen size and stiff middle lamellae. However, their low indentation modulus is due to a high microfibrillar angle, penalizing their longitudinal stiffness but making them interesting for impact or deformation performance. The two fabrics exhibit layers of preferred fibres orientations, quasi similar to unidirectional or +/-45° preforms, and hence may be used "as produced" as polymer reinforcements in technical composites but also in textile sector, in place of leather. Finally, their water uptake behaviour (21.2%-wt for Mutuba and 13.8%-wt for Kilundu) indicates opportunities for a range of environmentally-sensitive applications.

1. Introduction

Bark cloth making in Asia, Pacific Islands, Central and South America and Africa is one of humankind's oldest craft predating the invention of weaving. Indeed, the oldest bark cloth beater discovered recently in the South of China, dates back to 7898 ± 34 BP (Chang et al., 2015; Peña-Ahumada et al., 2020). The origin and spread of bark cloth tools also served as archaeological evidence to better understand human dispersal in the case of the Austronesian expansion. Several species from the Rosales family (Fig. 1) were used for bark cloth fabrication depending on the geographical area. In the Pacific Islands (primarily in Tonga, Samoa and Fiji, but as far afield as Niue, Cook Islands, Futuna, Solomon Islands, Java, New Zealand, Vanuatu, Papua New Guinea and Hawaii), paper mulberry was primarily used to produce "tapa cloth". The paper mulberry (*Broussonetia papyrifera*) is a species of flowering plant in the *Moraceae* family. Bark cloth was also occasionally made from *Artocarpus altilis*, *Ficus*, *Urticacecae* (nettle), *Hibiscus tiliaceus* or *Rubus* especially in Hawaii where it is called "kapa" (Di Tullio et al., 2020; Tamburini et al., 2019).

In Africa, the production of bark cloth fabric has been traditionally performed in Uganda since the thirteenth century. Fabrics are made from three species from the *Moraceae* family, mainly *Ficus natalensis* (Mutuba), *Ficus brachypoda*, and *Antiaris toxicaria* (Kilundu) (Rwawiire and Tomkova, 2017). The inner barks of trees are harvested during the wet season in the southern part of Uganda (Baganda) by manual peeling (Fig. 2a). The debarked stem is then covered with banana leaves for a

* Corresponding author.
E-mail address: alain.bourmaud@univ-ubs.fr (A. Bourmaud).

https://doi.org/10.1016/j.indcrop.2024.118613
Received 28 November 2023; Received in revised form 4 March 2024; Accepted 22 April 2024
Available online 27 April 2024

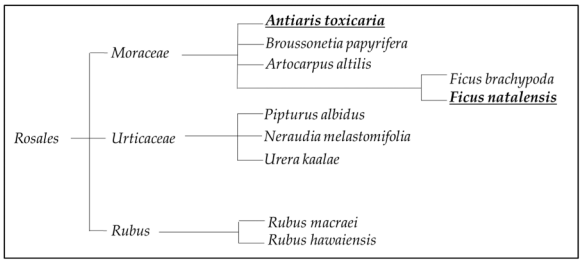

Fig. 1. Phylogenetic tree created from https://phylot.biobyte.de/. The two species analysed in the present article are highlighted in bold and underlined.

week to prevent dehydration and to allow the regrowth of fresh bark in a sustainable way. Meanwhile, the extracted fresh barks are heated for softening purposes before being subjected to a 'pummeling' process (Fig. 2b). It is beaten with different kinds of wooden mallets, giving different textures depending on the pace of the beats. A final sun-drying step results in its earthy terracotta colour. The fabric was worn by both men and women for cultural gatherings and for other domestic uses. The bark cloth of chiefs and kings could also be dyed in white or black. This craft was widely spread in every village, but the production slowed down with the growing availability of cotton introduced by Arab caravan traders during the nineteenth century. In recent years, the promotion of this traditional craft was encouraged, and it has been inscribed since 2008 in the Representative List of Intangible Cultural Heritage of Humanity in order to preserve its cultural legacy (Venkatraman et al., 2020; Walusimbi, 2001). Today, these bark products are being considered for the shoe industry, in place of leather.

Although the craft of bark cloth making is an ancestral know-how, scientific studies concerning its composition and structure are very limited. The present article aims at better understanding the nature and properties of these naturally occurring fabrics focusing on the case study of two bark cloths (Mutuba and Kilundu). The material characterisation will help ascertain their potential use in value-added applications such as in modern composites. Both bark cloth fibres are compared to other well-characterised plant fibres used in the composite industry (e.g. flax (bast) and sisal (leaf) fibres). We also compare the bark cloth fibres to date palm fibres, which also form naturally at the external surface of leaf sheaths in date palm trees, and therefore are an appropriate benchmark for these bark cloth fibres and textiles.

2. Materials and methods

2.1. Materials

Barks from "Mutuba tree" (*Ficus natalensis*) and "Kilundu tree" (*Anitaris toxicaria*) originate from Bulami (Wakiso district, Uganda). Both barks were collected at the same stages (6–7 months before manual peeling). The manual extraction of barks, the pummeling process and macroscopic samples are illustrated in Fig. 2.

2.2. Biochemical analysis

Prior to biochemical analysis, an Alcohol-Insoluble Material (AIM) was obtained after boiling fibres for 20 min in 70% ethanol (15 g/250 ML) (Gautreau et al., 2022). AIM was transferred to a G2 sintered glass filter, and the alcohol was removed by aspiration under vacuum. AIM was washed several times with 70% ethanol and then twice with absolute ethanol for 30 min. Finally, AIM was dried with acetone prior storage for the following biochemical investigations: lignin, monosaccharide and thioacidolysis (Gautreau et al., 2022). The extractives (i.e. low molecular weight molecules not bonded to the cell wall) were removed. Further, homogenization of the samples was performed by cryogrinding (SPEX 6700 freezer Mill) the AIM under liquid nitrogen to get powder. All results are expressed as a percentage of dry matter.

2.3. Cell wall monosaccharides

The raw powders were subjected to hydrolysis in 12 M H2SO4 (Sigma Aldrich) during 2 hours at 25°C. This step mainly hydrolyses cellulose. After addition of inositol used as an external standard, hydrolysis was continued in 1.5 M H2SO4 during 2 hours at 100°C. The resulting alditol acetate derivatives of the neutral sugars were analysed by gas phase chromatography (Perkin Elmer, Clarus 580, Shelton, CT, USA) equipped with a DB 225 capillary column (J&W Scientific, Folsorn, CA, USA) at 205 °C, with H2 as the carrier gas and a flame ionisation detector. Standard sugar solutions of known concentrations were used for calibration. Uronic acids (galacturonic and glucuronic acids) were determined by a colorimetric quantification (Blumenkrantz and Asboe-Hansen, 1973; Thibault, 1979). At least three independent assays were performed for each sample type.

2.4. Lignin

The lignin content was quantified by spectrophotometry following acetyl-bromid hydrolysis (Hatfield and Fukushima, 2005). Three independent assays were performed for each batch and the chemicals were

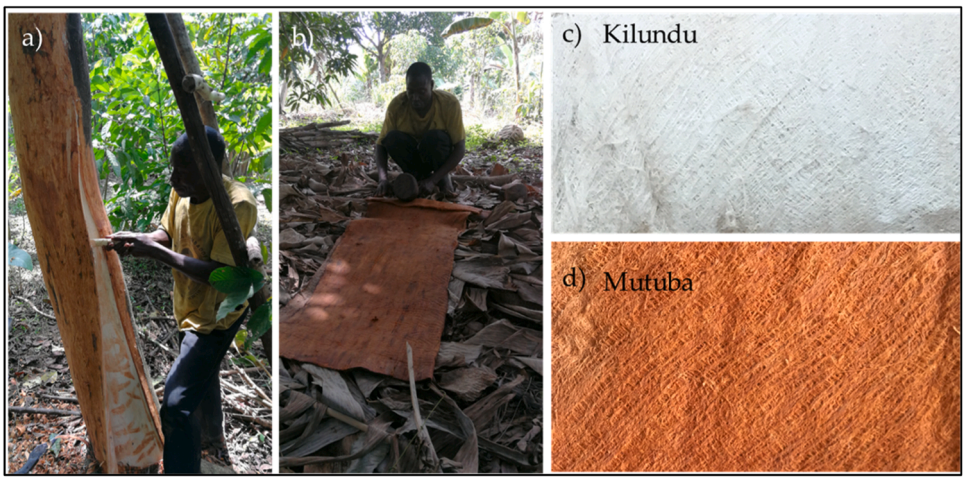

Fig. 2. a) Bark's manual extraction; b) pummeling process with a wooden beater; c) detail of the different samples with their name.

laboratory grade from Sigma Aldrich.

Lignin depolymerization was performed using thioacidolysis and subsequent gas chromatography-mass spectrometry. Thioacidolysis was used to determine beta-O-4 linked units in lignins of both species according to the method described in Lapierre et al. (Lapierre et al., 1985). Two independent assays were performed for each batch of samples. In addition, pyrolysis coupled to GC-MS was performed.

Pyrolysis-gas chromatography/mass spectrometry (Py-GC/MS) analysis was conducted using a CDS model 5250 pyroprobe autosampler connected to an Agilent 6890/5973 GC/MS system. The cellulose and wood (CW) samples weighing approximately 300 μg were subjected to pyrolysis inside a quartz tube at a temperature of 500°C for a duration of 15 seconds. Subsequently, the pyrolysis products were separated on a capillary column (5% phenyl methyl siloxane, 30 m, 250 μm i.d., and 0.25-μm film thickness). Helium was utilized as the carrier gas, flowing at a rate of 1 ML/min. The pyrolysis and GC/MS interfaces were maintained at a temperature of 290°C. The GC temperature program started at 40°C for 1 minute, followed by an increase of 6 °C/min to reach 130°C, then a further increase of 12 °C/min to reach 250°C, and finally a rapid increase of 30 °C/min to reach 300°C, where it was held for 3 minutes. The identification of various phenolic pyrolysis compounds was accomplished by comparing their spectra to previously published data (Ralph and Hatfield, 1991).

2.5. Wide-angle X-ray diffraction

Two independent assays were performed for each batch in environmental conditions on a Siemens D500 diffractometer with a CuKα radiation. The samples were placed on a silicon wafer and scans were collected for $2\theta = 10^{\circ}$ to 40° with a step of 0.03° and 2 s, at 30 kV and 20 mA. The crystallinity rate was calculated thanks to Ségal et al. (Segal et al., 1959) with the following equation were I_{tot} is the total intensity of the primary peak of cellulose I (at $2\theta \approx 22.5^{\circ}$), I_{am} is the intensity of the amorphous part defined as the minimum intensity at $2\theta \approx 18.5^{\circ}$.

$$C = \frac{I_{tot} - I_{am}}{I_{tot}} * 100 \quad (1)$$

2.6. Dynamic Vapour Sorption (DVS)

The sorption and desorption isotherms for water were established with a dynamic vapour sorption device (IGAsorpt-HT, idden Isochema, Warrington, UK). Samples of 25 mg of each fabric was placed in a microbalance located in the hermetic reactor. Prior to adsorption, the samples were dried at 105 °C for 1 h. Inside the reactor, the temperature and relative humidity (RH) were controlled. The sorption/desorption sequence was programmed as follows: an increase from 0% to 90% RH, and then decrease to 0% RH with 10% RH steps. For each RH step, the sample mass was continuously measured until reaching equilibrium, i.e. when the mass variation became less than 0.1 μg/min over 1 h.

2.7. Scanning electron microscopy and image analysis

The barks were observed by Scanning Electron Microscopy (SEM) using a Jeol JSM 6460LV microscope (France). Each sample was sputter coated with gold prior to the image acquisition. Several magnifications were selected for each sample. Preferential orientation of fibres was analysed by computing the histogram of pixels preferred orientations using grey-level granulometry. More details about the method can be found in (Gager et al., 2019; Melelli et al., 2020b; Richely et al., 2022). The measured orientations should be considered as relative values, as the orientation of the image with respect to the main axis of the tree was not referenced. Therefore, values should not be interpreted according to the angle values, but rather according to the number and width of the peaks that can be identified on the histograms.

2.8. Atomic Force Microscopy

The fibre bundles from each batch were extracted manually from the barks. They were embedded in a low viscosity resin (epoxy agar low viscosity resin (LV); Agar scientific; UK) and stored in an oven overnight at 60°C for the final polymerization. The resulting samples were cut transversally using an ultramicrotome (Leica EM UC7, Leica Microsystems SAS, Nanterre, France) equipped with glass and diamond knives (Histo and Ultra, Diatome, Nidau, Switzerland). Peak-Force Quantitative Nano-Mechanical property mapping (PF-QNM) was performed using a multimode 8 at. force microscope (Bruker) equipped with a RTESPA-525 probe (Bruker AFM Probes, Camarillo, CA, USA). The tip was calibrated using a relative method and the averaged normal spring constant was calculated using the Sader method (https://sadermethod.org/). The resonance frequency was set from between 507 and 547 kHz and the tip radius between 15 and 40 nm. Moreover, the peak force set-point was of 200 nN. Image processing was performed on Gwyddion software (http://gwyddion.net) and a detailed protocol can be found in Melelli et al. (Melelli et al., 2020b).

2.9. Finite element computation

Finite element computation is considered to gain insight on the ultrastructural role on the deformation mechanisms under elasticity behaviour of both Kilundu and Mutuba samples. AFM images are used as a basis for the 2D ***local mechanical mapping*** analysis. The images are converted into a finite element mesh using plane elements capable of displacement in X and Y directions. The size of the model is equal to the resolution of the images, which represents 262,144 elements, corresponding to 526,338 degrees of freedom (dof).

Elastic material properties are implemented according to AFM mapping allowing to capture the heterogenous distribution of stiffness for both samples. The boundary conditions correspond to in-plane tensile loading conditions, where for instance a loading in X direction generates a constrained edge against displacement (UX=UY=0) at X=0 and a displacement imposed in X-direction by a fixed amount (UY=0, UX=0.05×L at x=L, where L= 20 μm).

The elasticity problem is solved using a preconditioned gradient method.

3. Results and discussion

3.1. Composition and ultrastructure

Mutuba presents a significantly higher content of cell wall monosaccharides released after hydrolysis than Kilundu, i.e. 71.1 ± 3.0% compared to 57.8 ± 3.6% (Table 1 and Fig. 3). This difference is mainly explained by an elevated glucose content in Mutuba (52.0 ± 1.7% and 37.9 ± 1.9% for Mutuba and Kilundu respectively), and therefore cellulose content. Rwawiire et al. (Rwawiire, 2016). observed an even higher cellulose content for Mutuba (69%) than in the present study (52%). This difference can be explained by varied growing conditions and extraction methods. The cellulose content is lower in both bark types compared to flax fibres (between 60% and 85%) as reported in literature (Bourmaud et al., 2019a; Mayer-Laigle et al., 2020). However, cellulose content is in the same range as for other plant fibres often used for reinforcements such as date palm, alfa, bamboo, coir or different species of wood, and in the low range of values reported for kenaf and sisal in the case of Mutuba (Bourmaud et al., 2018, 2017). For both bark cloth fibres, galacturonic acid content is around 9% (9.6 ± 0.4 and 9.2 ± 0.5 for Mutuba and Kilundu respectively), highlighting a significant pectin content comparable to the values reported for kapok or sisal, for instance (Bourmaud et al., 2018). The other monosaccharides are minor, but one can notice significantly higher xylose and galactose contents for Mutuba compared to Kilundu, and significantly higher arabinose and glucuronic acid contents for Kilundu compared to Mutuba. These data

Table 1
Cell wall monosaccharide contents released by hydrolysis as a function of dry matter (%) of Mutuba and Kilundu. glcA = glucuronic acid, galA = galacturonic acid, xyl = xylose, glc = glucose, gal = galactose, rha = rhamnose, ara = arabinose, man = mannose.

Sample	Total	Glc	GalA	Xyl	Ara	Gal	GlcA	Rha	Man
Mutuba	71.1 ± 3.0	52.0 ± 1.7	9.6 ± 0.4	3.9 ± 0.2	1.9 ± 0.0	1.8 ± 0.1	0.4 ± 0.3	0.9 ± 0.3	0.7 ± 0.1
Kilundu	57.8 ± 3.6	37.9 ± 1.9	9.2 ± 0.5	3.3 ± 0.1	3.2 ± 0.1	1.3 ± 0.1	1.3 ± 0.5	0.8 ± 0.1	0.6 ± 0.1

Table 2
Lignin content obtained by acetyl-bromid method and results of thioacidolysis (yields and % of lignin-derivated monomers of H, G and S types). The yields are expressed in μmol/g of sample.

Technique	Acetyl-bromid	Thioacidolysis					
Sample	Lignin (%)	G yield (%)	S yield (%)	(H+G+S) yield (%)	%G	%S	S/G
Mutuba	10.2 ± 0.2	9.3 ± 0.5	11.3 ± 0.6	20.6 ± 1.1	45.2 ± 0.1	54.8 ± 0.1	1.21 ± 0.0
Kilundu	2.7 ± 0.3	2.9 ± 0.0	9.8 ± 0.1	12.7 ± 0.1	23.0 ± 0.0	77.0 ± 0.0	3.35 ± 0.00

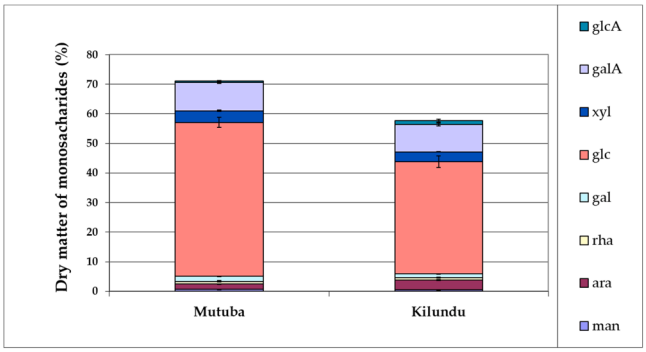

Fig. 3. Different monosaccharide contents as a function of dry matter (%). glcA = glucuronic acid, galA = galacturonic acid, xyl = xylose, glc = glucose, gal = galactose, rha = rhamnose, ara = arabinose, man = mannose.

suggest substantial differences in hemicelluloses between the two species. Acetyl-bromid analyis highlights a lower lignin content for Kilundu compared to Mutuba (10.2 ± 0.2% for Mutuba and 2.7 ± 0.3% for Kilundu). Higher lignin content, and also the sun-drying process may explain the richer brown/reddish colour observed in Mutuba (Fig. 2d).

Acetyl-bromid analysis highlights a lower lignin content for Kilundu compared to Mutuba (10.2 ± 0.2% for Mutuba and 2.7 ± 0.3% for Kilundu). Higher lignin content, and also the sun-drying process may explain the richer brown/reddish colour observed in Mutuba (Fig. 2d). Interestingly, the lignin content of Mutuba fibres is similar to Abaca fibres and in the lower range of jute or sisal (Bourmaud et al., 2018), whereas the lignin content of Kilundu is closer to content observed in flax, hemp or ramie.

In both cases the lignin content is lower than date palm fibres, with values reported around 17% (Bourmaud et al., 2017). Lower lignin content of Kilundu compared to Mutuba fabrics is confirmed by thioacidolysis, with yields of respectively 12.7 and 20.6 μmol / g of sample. In comparison, thioacidolysis of poplar wood provides a yield close to 500 μmol / g (with a total lignin content of about 20%) and 300 μmol/g for a conifer wood such as spruce (with a lignin rate close to 28%). The low thioacidolysis yield in both bark cloths highlights very few labile Beta-O-4 bonds.

Lignins are mainly composed of *p*-hydroxyphenyl (H), guaiacyl (G) and syringyl (S) units and their relative abundance depend on their *in-situ* localization. For instance, lignins in vessels are usually made of G units while fibre lignins are rich in S units. In these fibre-rich bark lignins, the proportion of thioacidolysis-released S units is high compared to G units (Fig. 4). The prevalence of S units compared to G units was

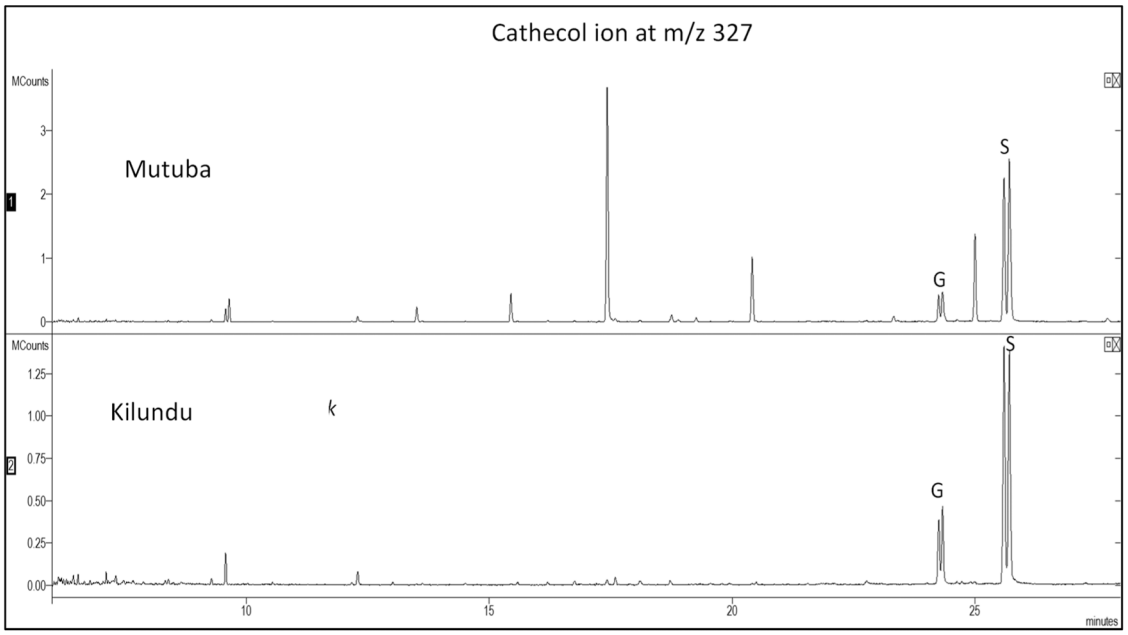

Fig. 4. Chromatogram of thioacidolysis compounds by GC/MS.

confirmed by analytical pyrolysis, showing higher peaks attributed to S units. Interestingly, colour presence of tannins in Mutuba bark is also observable by pyrolysis (Fig.S.1). Indeed, peaks corresponding to C-catechol and C-4-methylcatechol where clearly identified in Mutuba bark cloth and not in Kilundu. High concentration of condensed tannins (proanthocyanidins) may further explain the red color observed in Mutuba (Fig. 2d).

Biochemical analyses are scarce in literature for Mutuba and Kilundu back cloths. Rwawiire et al. (Rwawiire, 2016) determined a higher lignin content (15%) for Mutuba than the values we report here (10.2 ± 0.2%) but it is difficult to compare these data because different experimental methods were used in both studies. Moreover, as highlighted by our results, the bark of Mutuba is rich in condensed tannins and these condensed tannins are likely to be counted as acid-insoluble lignin in the Klason assay, possibly explaining the higher lignin content depicted in their results. The rate of condensed tannins can indeed be very high in the barks (5–50% (Fengel and Wenzkowski, 1986)).

The ultrastructure of plant fibres plays an important role in their mechanical properties, influencing both stiffness and strength. It refers mainly to cellulose with two major parameters: the crystallinity rate and the orientation of the microfibrils according to the normal axis of the fibre in the secondary cell wall, also called the microfibril angle (MFA).

In the present work, the curves obtained from X-ray diffraction of Mutuba and Kilundu confirm the presence of amorphous and crystalline cellulose I (Fig. 5). The cellulose crystallinity index is significantly higher for Mutuba compared to Kilundu, with values of 76.6 ± 4.9% and 66.3 ± 0.5%, respectively. In both cases, the predominant amount of crystalline cellulose is in favour of high mechanical properties and appears in the same range as flax, with values reported between 70% and 85%, and higher than date palm fibres, with values of 41 ± 3% reported by Bourmaud et al. (Bourmaud et al., 2019b). The precise estimation of the MFA could be conducted in the future thanks to Synchrotron X-ray diffraction, second harmonic generation or transmission ellipsometry microscopies for instance (Richely et al., 2022), to better predict the fibre mechanical properties. The organization of the matrix components surrounding the cellulose microfibrils could also be investigated by Nuclear Magnetic Resonancy (NMR) for instance.

3.2. Potential use for composite applications

3.2.1. Hygroscopic behaviour studied plant fibres

The sorption / desorption behaviour of the different samples is displayed in Fig. 6. A difference in sorption capacity is observed between Kilundu and Mutuba above 10% of Relative Humidity (RH), reaching respective mass difference of 13.8 and 21.2% at 90% RH. Mutuba seems more sensitive to changes, possibly due to higher cellulose content, in

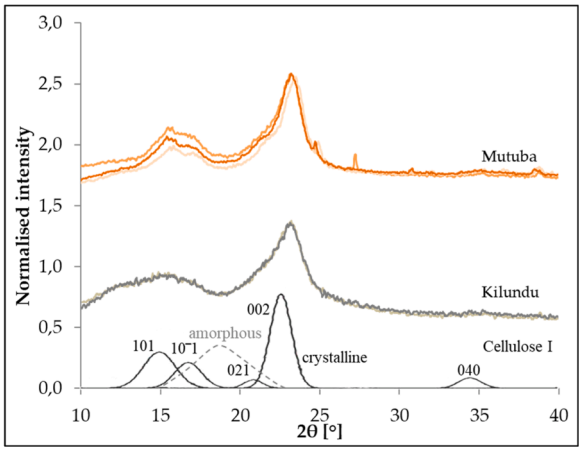

Fig. 5. Wide-angle X-ray diffraction curves from the Kilundu and Mutuba samples.

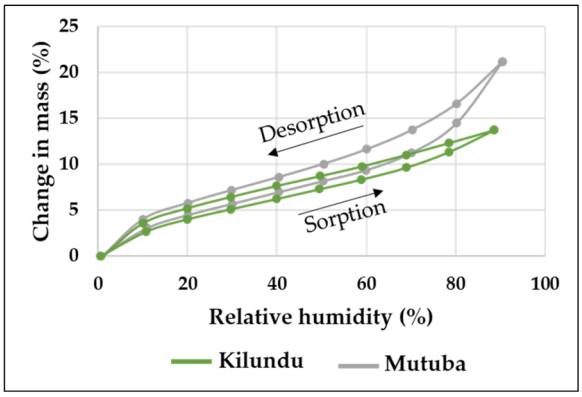

Fig. 6. Comparison of sorption / desorption curves for Kilundu and Mutuba samples.

hygroscopic conditions above 10% RH, possibly due to higher cellulose content, but is still in the lower range of results obtained by Garat et al. and Bourmaud et al. (Bourmaud et al., 2017; Garat et al., 2020) on different plant bundles. Moisture content between 15% and 30% were indeed obtained by DVS for flax, hemp, palm, sisal, date palm and nettle bundles at 90% of relative humidity, the latter being increasingly hydrophilic. Regarding hysteresis, the fact that sorption and desorption curves of most natural fibres are not superimposable has been well described in literature (Hill et al., 2009).

Up to 10% RH, the adsorption properties are mostly linked to the composition and crystallinity of the fibres. Indeed, at low %RH water is principally absorbed through hydrogen bonding by amorphous cellulose and hemicellulose in the inner-most cell wall layer, until saturation. In the present case, Kilundu presents a lower hydrophobic lignin content and crystallinity rate compared to Mutuba. It is in favor of a higher moisture content for Kilundu compared to Mutuba, but the phenomena might be counterbalanced by the higher overall cellulose content; explaining the similar sorption behavior up to 10% RH between Kilundu and Mutuba.

Between 10% and 60% RH, the porous structure of the fibres and cell wall enables absorption of water into the other cell wall layers through micro-capillaries. Above 60% RH, capillary condensation dominates, and water molecules aggregate to form a fluidic, bulk phase. Differences between Mutuba and Kilundu are very high at high %RH (above 60%). Other features such as structural and morphological parameters might influence the water sorption and swelling of the fabrics at high %RH (Garat et al., 2020).

As evidenced by Garat et al. (Garat et al., 2020), variations of water uptake and swelling behaviour were observed at the bundle scale depending on biochemical and structural characteristics of the plant species studied. The hygroexpansion coefficients estimated in their study seem negatively correlated to the lignin content and MFA. In the prospect of composite applications, the hygroscopic nature of the fibres does not prevent their use for composite applications, as it is also the case for flax and hemp already widely employed in composites. Best practice guidelines have been formulated to cope with this characteristic of most plant fibres depending on their final use environment (i.e. indoor, outdoor or immersed conditions) and also of the processing parameters, a better durability being reached when hydrophilic fibres are fully embedded in the polymer matrix and when porosity degree is reduced at maximum.

3.2.2. Naturally occurring fabrics with preferred fibre orientations

A distinctive and remarkable property of Kilundu and Mutuba fibres compared to other plant fibres for composite applications is that they are naturally organized into an oriented non-woven fabric within the bark of the tree (Fig. 7). A single preferred orientation is highlighted for Mutuba sample, representing approximatively 75% of the fibre content. In the

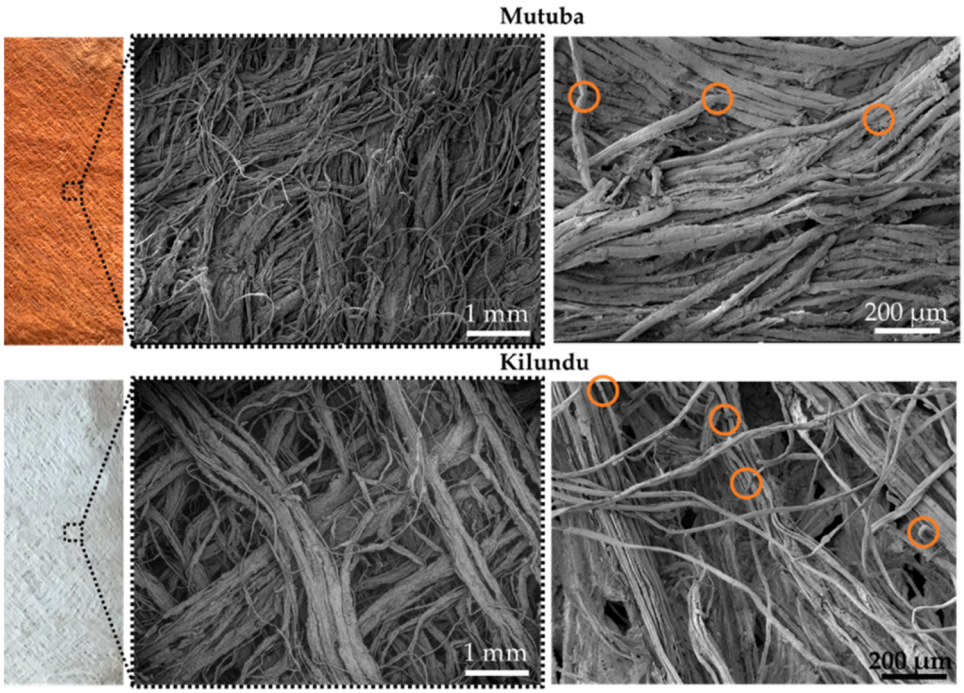

Fig. 7. Macroscopic (left) and SEM images (middle and right) of the surface of the Mutuba and Kilundu barks, with three different magnifications. Orange circles underline the presence of defects (visible cracks, twists or bends).

case of Kilundu, two main orientations exist, similar to a +/- 45° preform (Fig. 8), even though variations exist, according to the considered preform side (top, bottom) of the product. However, one should keep in mind that the present observations are representative of the surface of the sample, and that the structure may be layered with other preferential fibre orientations within its thickness, similarly to a fabric.

Surface roughness measurements using a non-contact profilometer for instance could be of interest to compare the present roughness to the one from fibres already widely used for composite applications such as flax and hemp. As the fibres and bundles are already assembled into a fabric, special caution should be addressed to the composite processing parameters to obtain sufficient resin impregnation (Pantaloni et al., 2020).

The presence of defects arising from the mechanical extraction of the bundles from the stems were largely described in literature (Bourmaud et al., 2022; Richely et al., 2021) in the case of flax and hemp. Hugues et al. (Hugues et al., 2000) evidenced stress concentrations at the matrix-fibre interphase of hemp-epoxy composites eventually leading to their failure. In the case of Mutuba and Kilundu bark cloths, some defects are underlined by orange circles in Fig. 7; in the form of twisting, bending or even visible cracks. The influence of the manual peeling-off and pummelling processes on the creation of defects should be further investigated, for instance with the help of X-ray microtomography to observe additional porosities or lumen disruption. It will enable to adapt, if necessary, the process initially designed for textiles to prevent the appearance of defects and fulfil composite requirements, as much as possible.

3.2.3. *Cell wall mechanical characterisation*

Most plant fibres are linked by a middle lamella (ML), rich in pectin, lignin and proteins, which is strongly bonded to the primary cell walls, forming the compound middle lamella (CML) (Zamil and Geitmann, 2017). In the case of Mutuba and Kilundu, a CML is clearly identified close to the fibres (Fig. 9). Regarding its morphology, it is usually difficult to distinguish the middle lamella from the main cell walls, as noticed for Kilundu sample. In the case of Mutuba, the fibres seem individualized and the CML appears to be dissociated from the main cell wall.

However, as no mechanical gradient corresponding to internal sublayers is observed within the cell walls, it is therefore difficult to conclude whether the failure occurred at the interface between cell wall sublayers, as has been observed in numerous studies (Melelli et al., 2020a), or at the interface between the ML and primary cell walls. In the case of Kilundu, some fibres are still bonded together with the presence of the CML at the interface; and the two adjacent primary cell walls can be distinguished. In addition, three internal sublayers are revealed by concentric borders (Fig. 8-bottom), showing an internal structure close to the model usually attributed to plant fibres such as flax, with a secondary wall divided in three sublayers (Bourmaud et al., 2018). Successive layers can also be induced, in the same cell wall, due to the progressive deposition of cellulose during the biochemical synthesis of the wall.

Traces of internal porosity, called lumen, are observed for both Kilundu and Mutuba fibres. Despite a possible deformation of the lumen during sample preparation, we can conclude that the lumen only represents a small fraction of the cross-sectional area for all samples, suggesting an important mechanical function for these cell walls.

The indentation moduli seem uniform within the cell walls for both samples, with mean values of 7.2 ± 0.7 GPa and 8.4 ± 0.9 GPa for Mutuba and Kilundu, respectively. These values are almost three times lower than for flax, with indentation modulus of 21.2 ± 2.2 GPa described in literature, two times lower than date palm fibres and closer to the indentation modulus of tension wood for instance. In literature, the longitudinal nanoindentation modulus of mature plant cell walls is indeed generally depicted between 15 and 22 GPa and is usually comparable to the indentation modulus obtained by AFM (Bourmaud et al., 2018). Biochemical composition, namely cellulose content, and structural arrangement of the biopolymers within the cell walls could explain these differences, and especially the microfibril angle (MFA). The orientation of the cellulose microfibrils within the cell walls with respect to the fibre axis is indeed a crucial parameter influencing greatly the mechanical properties of the fibres and should be studied by Synchrotron X-ray diffraction for instance. According to the method developed by Jäger et al. (Jäger et al., 2011), it is possible to estimate the MFA of

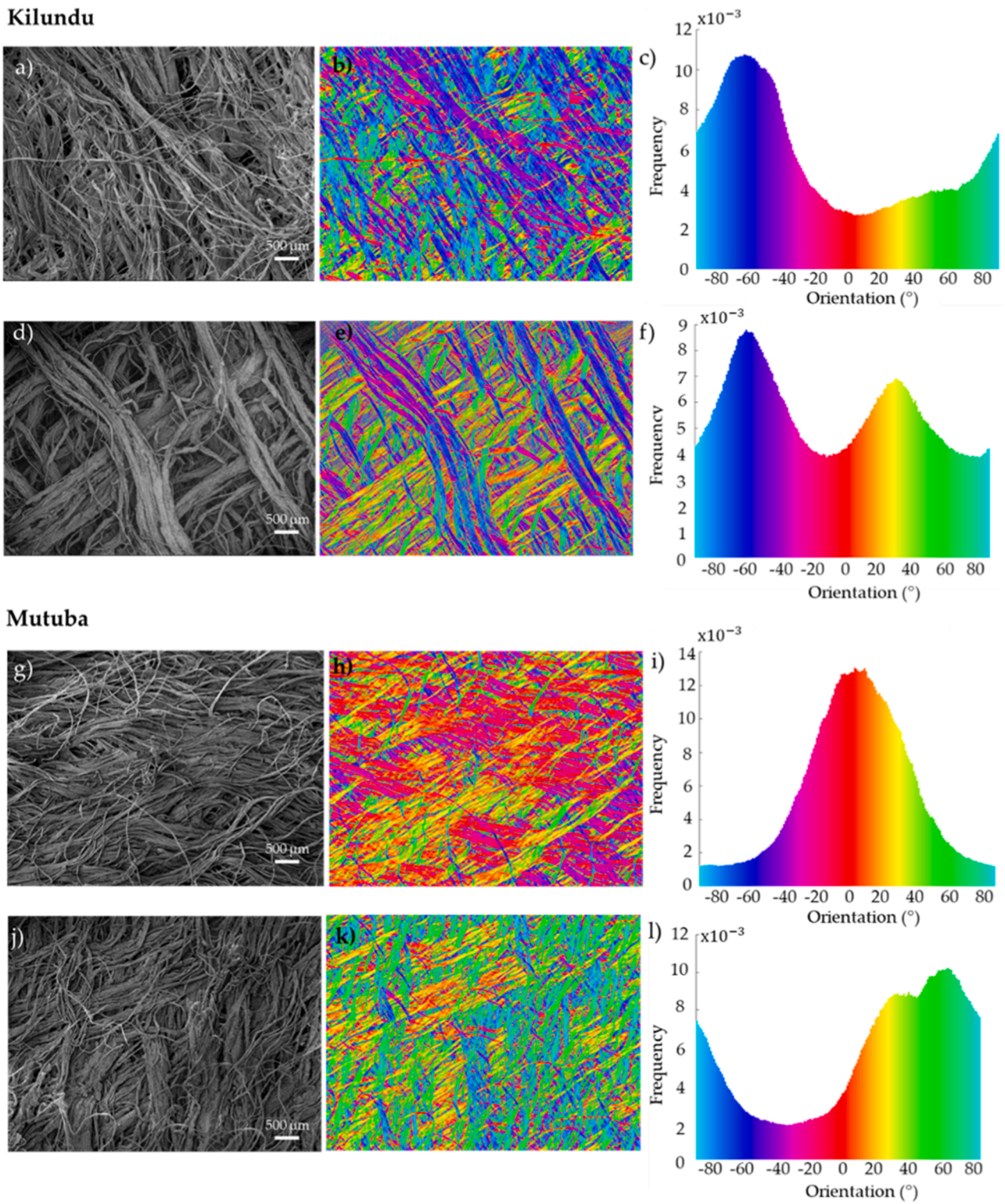

Fig. 8. a), d), g) and j): Original images; b), d), h) and e) k): Colour representations of preferred orientation map; c), f), i) and l): histograms of preferred orientations for two Kilundu and Mutuba samples.

the fibres, knowing the cellulose content. For cellulose values around 40 or 50% and indentation modulus of 7–9 GPa, the MFA would be around 60–70° which is very high but possible. This inverse method must be considered with caution but enables a quick estimation of the MFA. The active mechanical contribution of inner bark fibres organized in a trellis structure to the straight growth of trees have been described in literature (Clair et al., 2018), highlighting their role of mechanical support within the trees. Despite the low indentation moduli observed in the present study, Rwawiire et al. (Rwawiire et al., 2015) revealed strength values fulfilling requirements for applications as interior automotive panels in the form of bark cloth reinforced green epoxy biocomposites.

The indentation moduli of the CML are not significantly different for Mutuba and Kilundu: 6.6 ± 0.5 GPa and 7.0 ± 0.6 GPa respectively, despite a higher global lignin content observed for Mutuba compared to

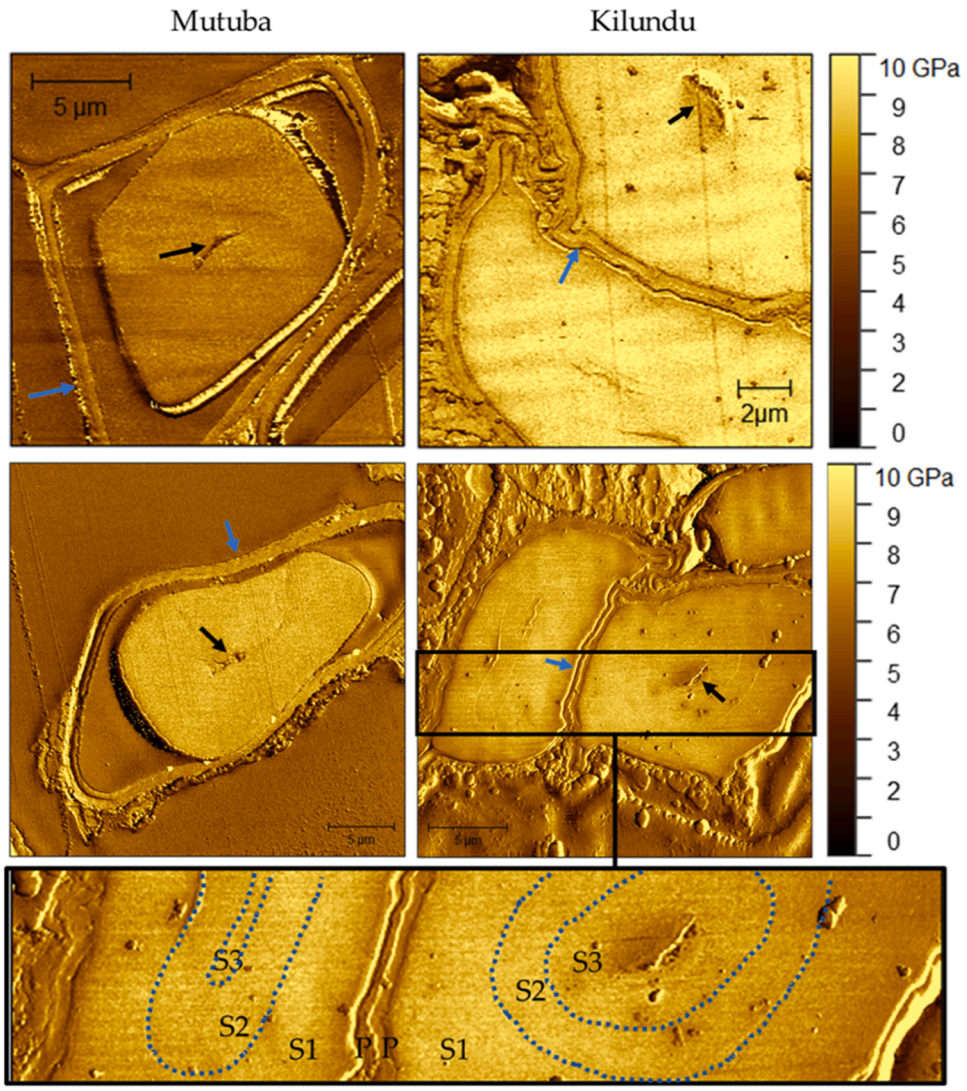

Fig. 9. Indentation modulus mappings of each sample type. The blue arrows highlight middle lamellas, dark arrows report the traces of an internal porosity (lumen). An internal structure is visible only on the Kilundu samples, showing concentric sublayers that are underlined in blue dotted lines on the bottom picture.

Kilundu. A local biochemical analysis could help better understanding the lignin localization. In the prospect of composite applications, the CML is an important feature in the mechanical properties of the final material (Beaugrand et al., 2017). In the case of Kilundu and Mutuba, the indentation moduli of the cell walls and middle lamella are closer than for flax, which exhibit a CML indentation modulus more than two times lower than within its cell walls (10.2 ± 1.2 GPa). As mentioned by Melelli et al. (Melelli et al., 2020a), it is difficult to directly correlate the indentation modulus of the CML to the mechanical properties and damage mechanisms of the bundles in the biocomposites. The morphology, biochemical composition and structure of the fibres, bundles, and fabrics should not be neglected. It is important to ask the question of the relevant scale of mechanical characterization needed in order to design composite materials. In addition to the cell wall scale, the fibre and/or bundle scale are usually studied for plant fibre reinforcement to get a global overview of the mechanical properties. The resulting information is complementary to the one obtained at the cell wall scale, including the effect of the MFA, internal porosities, geometry of the fibre, the thicknesses of the cell walls and the role of the middle lamella. In our case, fibres are originally forming a fabric, it could naturally be of interest to get accurate information at this reinforcement unit scale in future work, as well as deepen the knowledge at the composite scale.

3.2.4. Insights on the prediction of elasticity behaviour at the microstructural level

As discussed in Section 2.7, finite element computations rely on the conversion of the indentation moduli maps (Fig. 9) into finite element meshes where the heterogenous structure is imbedded into 2D elasticity model. Tensile conditions are simulated in both X (horizontal) and Y (vertical) directions. The resulting stress distributions for an extension of 5% in both direction is discussed Fig. 10 shows the predicted von Mises stress distributions for both Kilundu and Mutuba samples for uniaxial loading conditions corresponding to 5% of overall strain.

These results are achieved from the implementation of material property distributions retrieved from AFM analysis (Fig. 9). The results show contrasted situations related to higher stress levels predicted in the case of Kilundu samples. This trend irrespective of the loading direction highlights the differences in terms of stiffness between the samples illustrated in Table 3. In both cases, stress heterogeneity develops which is not compatible with the uniformity of the indentation moduli. This heterogeneity is also not related much to the presence of the lumen. However, it is more related to differences between the concentric sublayers. The origin of such heterogeneity is explained by the role of the interface between the ML and primary cell walls. High stress levels are depicted at the positions where large stiffness gradients are observed. In terms of anisotropy behaviour, the two samples do not exhibit a strong

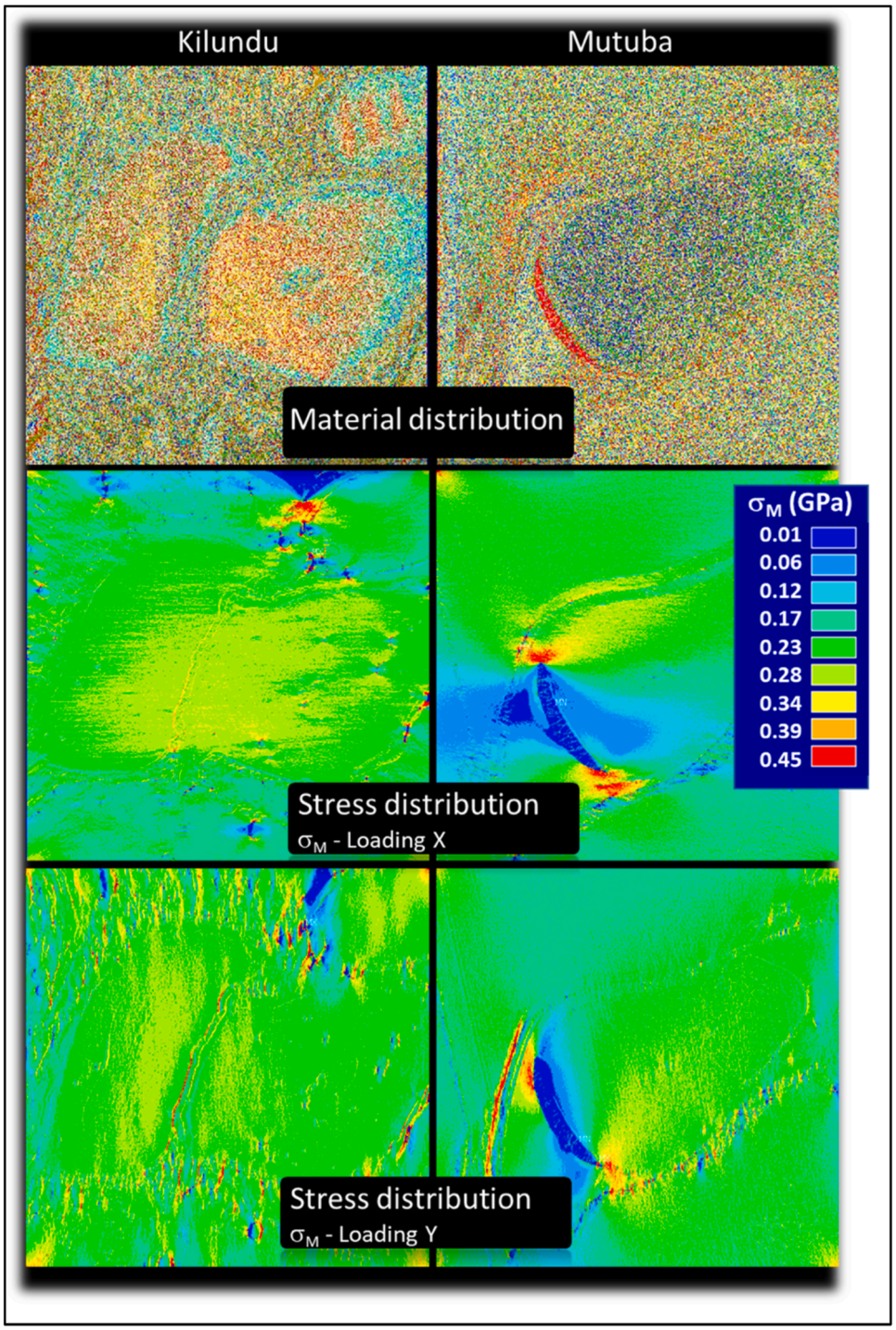

Fig. 10. Finite element simulation results compared for Kilundu and Mutuba samples based on uniaxial loading in X and Y directions. Material distributions and von Mises stress counterplots.

dependence on the direction of testing. The ratio between the moduli of elasticity in X and Y directions are 0.95 and 0.92 for Kilundu and Mutuba, respectively. The average longitudinal Young's modulus measured for both samples is 6.14 GPa and 5.58 GPa, respectively. This places the stiffness of Kilundu 15% above that of Mutuba.

4. Concluding discussion

The present work investigated the structure and properties of ancestral and naturally occurring fabrics from two bark trees of Uganda ("Kilundu": *Antiaris toxicaria* and "Mutuba": *Ficus natalensis*) in order to determine their potential use as locally-available, low-cost composite reinforcements. Table 4 synthesises the properties and main characteristics we measured for Mutuba and Kilundu, compared to those of a common reinforcement used in composite industry (flax) and another original plant product, also available as a fabric preform in Nature, date palm leaf sheath.

Structurally speaking, what is remarkable for the both studied tree bark cloth products are their cellulose content and properties and especially their high cellulose crystallinity degree, similar to flax fibres,

Table 3
Indentation modulus obtained by nanoindentation or AFM for Mutuba and Kilundu in the present work and comparison with values from literature (Arnould et al., 2017; Arnould and Arinero, 2015; Bourmaud et al., 2017; Tanguy et al., 2016). The number of measurements for Mutuba and Kilundu is specified in brackets.

Sample name	Cell wall indentation modulus (GPa)	CML indentation modulus (GPa)
Mutuba	7.2 ± 0.7 *(3)*	6.6 ± 0.5 *(3)*
Kilundu	8.4 ± 0.9 *(3)*	7.0 ± 0.6 *(2)*
Date palm leaf sheath	15.8 ± 2.4	6.7 ± 0.6
Flax	21.3 ± 2.2	10.2 ± 1.2
Kenaf	18.6 ± 1.5	10.2 ± 2.2
Jute	13.1–14.5	10.9 ± 1.6
Nettle	18–22	14.7 ± 1.3
Hemp	22–23	16.1 ± 1.4
Tension wood	11 or 15.1 ± 2.6	6.0 ± 0.5
Bamboo	21.3 ± 2.9	14.4 ± 3.6

Table 4
Summary of observations conducted in the present study on Mutuba and Kilundu barks, compared to flax and date palm fibre properties widely described in literature.

	Mutuba	Kilundu	Flax	Date palm leaf sheat
Glucose (% of dry mass)	52.0 ± 1.7	37.9 ± 1.9	60–85	45.1 ± 3.4
Uronic acids (%)	10 ± 0.4	10.5 ± 0.5	1–2	1.8 ± 0.2
Lignin (%)	10.2 ± 0.2	2.7 ± 0.3	1–3	16.9 ± 0.3
Crystallinity (%)	76.6 ± 4.9	66.3 ± 0.5	70–85	41 ± 3%
Water uptake at 90% RH (%)	21.2	13.8	18–20	24
Cell wall indentation modulus (GPa)	7.2 ± 0.7	8.4 ± 0.9	21.2 ± 2.2	16
CML indentation modulus (GPa)	6.6 ± 0.5	7.0 ± 0.6	10.2 ± 1.2	10–12
Scale after mechanical extraction	Fabric	Fabric	Bundle	Fabric

with values for Mutuba and Kilundu of 76.6 ± 4.9% and 66.3 ± 0.5%, respectively. In spite of this, local mechanical properties, at cell wall scale, remains low and are two to three times lower than indentation modulus reported for date palm and flax. This poor correlation between stiffness and cellulose content and crystallinity is unusual but, in the present case, explained by the low cellulose microfibrillar angle of the considered bark cloth fibres – this key parameter is strongly linked to the local stiffness measured through indentation tests.

The architecture of the two tissues exhibits pronounced specificities. A special attention was drawn to the compound middle lamella (CML) observed for both species. Further local biochemical analysis could help understand the localization of the abundant pectins (with uronic acids contents around 10%) and the differences of lignin content between Mutuba and Kilundu, with respective values of 10.2 ± 0.2% and 2.7 ± 0.3%; the latter being comparable to flax.

Finite element results confirm the experimental tendency where the average stiffness of Kilundu is 15% higher than that of Mutuba. Stress heterogeneity is found to develop at the regions of higher stiffness gradient, where the CML is observed to play a larger role in promoting stress localisation compared to the lumen. This point is preponderant for a future use of the preforms as composite reinforcements, the high stiffness and cohesion being positive for the alignment of fibre bundles in a polymer flow but counterbalanced by the poor fibre division ability. The natural weaving of the fibre bundles with one or two preferential orientations (+45°/-45°) revealed by surface image analysis is a tremendous advantage in terms of process-saving that should be underlined, as well as a great illustration of Nature's efficiency. A study of the cross-sections could be interesting in the future to better characterize the fabrics in terms of layers and thicknesses. Important parameters to ensure sufficient interfacial properties in the composites were identified, including surface roughness, individualization of the fibres and ease of impregnation of the resin. A careful attention to these parameters will be provided in future work. Low porosity contents were qualitatively revealed for both fibre types, in agreement with their possible role of support within the barks. Moreover, no internal sublayers were observed on the cross-sections of Mutuba, whereas the internal organization of the Kilundu secondary cell wall seems closer to the flax fibre model, with three sublayers of different thicknesses.

Both Kilundu and Mutuba present the typical hygroscopic behaviour of plant fibres, with a higher sensitivity to water uptake at high RH% for Mutuba, close to flax, compared to Kilundu. The choice of reinforcement might therefore be guided by these differences, especially for outdoor or immersed applications. Additional information at the cell wall scale (structural arrangement of the biopolymers within the cell walls), at the fibre scale (porosity and related defects, MFA) and at the fabric scale (roughness, mechanical properties) could be of interest to adapt the extraction processes if needed and guide the design of composites. The next steps will also include the manufacturing and testing of composites from these naturally-occurring reinforcements. In any case, the specific properties of the reinforcements highlighted here also demonstrate that the preforms can be used directly for the manufacture of objects such as leather goods, as a substitute for leather.

CRediT authorship contribution statement

Hom N Dhakal: Writing – review & editing. **Sofiane Guessasma:** Conceptualization, Formal analysis, Investigation, Writing – original draft, Writing – review & editing. **Richard Sibout:** Investigation, Methodology, Writing – review & editing. **Catherine Lapierre:** Investigation, Methodology, Writing – review & editing. **Emmanuelle Richely:** Writing – original draft, Visualization, Investigation, Conceptualization. **Sylvie Chevallier:** Investigation, Methodology, Writing – review & editing. **Delphin Pantaloni:** Conceptualization, Investigation, Methodology, Writing – review & editing. **Dieuveil Ngoubou:** Funding acquisition, Resources, Writing – review & editing. **David Legland:** Writing – review & editing, Methodology, Formal analysis. **Darshil U Shah:** Writing – review & editing, Validation, Conceptualization. **Guilhem Blès:** Writing – review & editing. **Sylvie Durand:** Writing – review & editing, Visualization, Methodology, Investigation, Conceptualization. **Johnny Beaugrand:** Writing – review & editing, Conceptualization. **Victor Gager:** Writing – review & editing, Methodology, Investigation, Formal analysis. **Camille Goudenhooft:** Writing – review & editing, Methodology, Investigation, Conceptualization. **Alain Bourmaud:** Writing – review & editing, Supervision, Project administration, Methodology, Funding acquisition, Conceptualization.

Declaration of Competing Interest

The authors declare that they have no known competing financial interests or personal relationships with other people or organizations that could have appeared to influence the work reported in this paper.

Data Availability

Data will be made available on request.

Acknowledgments

The authors want to thank the INTERREG IV Cross Channel programme for funding this work through the FLOWER project (Grant Number 23).

Appendix A. Supporting information

Supplementary data associated with this article can be found in the online version at doi:10.1016/j.indcrop.2024.118613.

References

Arnould, O., Arinero, R., 2015. Towards a better understanding of wood cell wall characterisation with contact resonance atomic force microscopy. Compos. Part A-Appl. Sci. 74, 69–76.

Arnould, O., Siniscalco, D., Bourmaud, A., Le Duigou, A., Baley, C., 2017. Better insight into the nano-mechanical properties of flax fibre cell walls. Ind. Crop. Prod. 97, 224–228. https://doi.org/10.1016/j.indcrop.2016.12.020.

Beaugrand, J., Guessasma, S., Maigret, J.-E., 2017. Damage mechanisms in defected natural fibers. Sci. Rep. 7, 14041 https://doi.org/10.1038/s41598-017-14514-6.

Blumenkrantz, N., Asboe-Hansen, G., 1973. New method for quantitative determination of uronic acids. Anal. Biochem. 54, 484–489.

Bourmaud, A., Beaugrand, J., Shah, D., Placet, V., Baley, C., 2018. Towards the design of high-performance plant fibre composites. Prog. Mater. Sci. 97, 347–408.

Bourmaud, A., Dhakal, H., Habrant, A., Padovani, J., Siniscalco, D., Ramage, M.H., Beaugrand, J., Shah, D.U., 2017. Exploring the potential of waste leaf sheath date palm fibres for composite reinforcement through a structural and mechanical analysis. Compos. Part A Appl. Sci. Manuf. 103 https://doi.org/10.1016/j.compositesa.2017.10.017.

Bourmaud, A., Mérotte, J., Siniscalco, D., Le Gall, M., Gager, V., Le Duigou, A., Pierre, F., Behlouli, K., Arnould, O., Beaugrand, J., Baley, C., 2019a. Main criteria of sustainable natural fibre for efficient unidirectional biocomposites. Compos. Part A Appl. Sci. Manuf. 124, 105504 https://doi.org/10.1016/j.compositesa.2019.105504.

Bourmaud, A., Pinsard, L., Guillou, E., De Luycker, E., Fazzini, M., Perrin, J., Weitkamp, T., Ouagne, P., 2022. Elucidating the formation of structural defects in flax fibres through synchrotron X-ray phase-contrast microtomography. Ind. Crops Prod. 184, 115048 https://doi.org/10.1016/j.indcrop.2022.115048.

Bourmaud, A., Siniscalco, D., Foucat, L., Goudenhooft, C., Falourd, X., Pontoire, B., Arnould, O., Beaugrand, J., Baley, C., 2019b. Evolution of flax cell wall ultrastructure and mechanical properties during the retting step. Carbohydr. Polym. 206, 48–56. https://doi.org/10.1016/j.carbpol.2018.10.065.

Chang, C.-S., Liu, H.-L., Moncada, X., Seelenfreund, A., Seelenfreund, D., Chung, K.-F., 2015. A holistic picture of Austronesian migrations revealed by phylogeography of Pacific paper mulberry. Proc. Natl. Acad. Sci. 112, 13537–13542. https://doi.org/10.1073/pnas.1503205112.

Clair, B., Déjardin, A., Pilate, G., Alméras, T., 2018. Is the G-Layer a Tertiary Cell Wall, 9, 8–11. https://doi.org/10.3389/fpls.2018.00623.

Di Tullio, V., Doherty, B., Capitani, D., Miliani, C., Greco, E., Ciliberto, E., Rossi, L., Proietti, N., 2020. NMR spectroscopy and micro-analytical techniques for studying the constitutive materials and the state of conservation of an ancient Tapa barkcloth from Polynesia, is. Wallis. J. Cult. Herit. 45, 379–388. https://doi.org/10.1016/j.culher.2020.02.009.

Fengel, D., Wenzkowski, M., 1986. Studies on Kapok 1. Electron Microscopic Observations. Holzforshung 40, 137–141.

Gager, V., Duigou, A., Le, Bourmaud, A., Pierre, F., Behlouli, K., Baley, C., 2019. Understanding the effect of moisture variation on the hygromechanical properties of porosity-controlled nonwoven biocomposites. Polym. Test. 78, 105944 https://doi.org/10.1016/j.polymertesting.2019.105944.

Garat, W., Le Moigne, N., Corn, S., Beaugrand, J., Bergeret, A., 2020. Swelling of natural fibre bundles under hygro- and hydrothermal conditions: Determination of hydric expansion coefficients by automated laser scanning. Compos. Part A Appl. Sci. Manuf. 131, 105803 https://doi.org/10.1016/j.compositesa.2020.105803.

Gautreau, M., Durand, S., Paturel, A., Le Gall, S., Foucat, L., Falourd, X., Novales, B., Ralet, M.-C., Chevallier, S., Kervoelen, A., Bourmaud, A., Guillon, F., Beaugrand, J., 2022. Impact of cell wall non-cellulosic and cellulosic polymers on the mechanical properties of flax fibre bundles. Carbohydr. Polym. 291, 119599 https://doi.org/10.1016/j.carbpol.2022.119599.

Hatfield, R., Fukushima, R.S., 2005. Can Lignin Be Accurately Measured?, in: Crop Science 45 (Ed.), Lignin and Forage Digestibility Symposium. 2003 CSSA, Denver, pp. 832–839.

Hill, C.A.S., Norton, A., Newman, G., 2009. The Water Vapor Sorption Behavior of Natural Fibers. J. Appl. Polym. Sci. 112, 1524–1537. https://doi.org/10.1002/app.29725.

Hugues, M., Sèbe, G., Hague, J., Hill, C., Spear, M., Mott, L., Hughes, M., Sèbe, G., Hague, J., Hill, C., Spear, M., Mott, L., 2000. An investigation into the effects of micro-compressive defects on interphase behaviour in hemp-epoxy composites using half-fringe photoelasticity. Compos. Interfaces 7, 13–29. https://doi.org/10.1163/156855400300183551.

Jäger, A., Bader, T., Hofstetter, K., Eberhardsteiner, J., 2011. The relation between indentation modulus, microfibril angle, and elastic properties of wood cell walls. Compos. Part A Appl. Sci. Manuf. 42, 677–685. https://doi.org/10.1016/j.compositesa.2011.02.007.

Lapierre, C., Monties, B., Rolando, C., de Chirale, L., 1985. Thioacidolysis of Lignin: Comparison with Acidolysis. J. Wood Chem. Technol. 5, 277–292. https://doi.org/10.1080/02773818508085193.

Mayer-Laigle, C., Bourmaud, A., Shah, D.U., Follain, N., Beaugrand, J., 2020. Unravelling the consequences of ultra-fine milling on physical and chemical characteristics of flax fibres. Powder Technol. 360 https://doi.org/10.1016/j.powtec.2019.10.024.

Melelli, A., Arnould, O., Beaugrand, J., Bourmaud, A., 2020a. The middle lamella of plant fibers used as composite reinforcement: Investigation by atomic force microscopy. Molecules 25. https://doi.org/10.3390/molecules25030632.

Melelli, A., Jamme, F., Legland, D., Beaugrand, J., Bourmaud, A., 2020b. Microfibril angle of elementary flax fibres investigated with polarised second harmonic generation microscopy. Ind. Crops Prod. 156, 112847 https://doi.org/10.1016/j.indcrop.2020.112847.

Pantaloni, D., Bourmaud, A., Baley, C., Clifford, M.J., Ramage, M.H., Shah, D.U., 2020. A review of permeability and flow simulation for liquid composite moulding of plant fibre composites. Materials 13. https://doi.org/10.3390/ma13214811.

Peña-Ahumada, B., Saldarriaga-Córdoba, M., Kardailsky, O., Moncada, X., Moraga, M., Matisoo-Smith, E., Seelenfreund, D., Seelenfreund, A., 2020. A tale of textiles: Genetic characterization of historical paper mulberry barkcloth from Oceania. PLoS One 15, 1–20. https://doi.org/10.1371/journal.pone.0233113.

Ralph, J., Hatfield, R.D., 1991. Pyrolysis-GC-MS characterization of forage materials. J. Agric. Food Chem. 39, 1426–1437. https://doi.org/10.1021/jf00008a014.

Richely, E., Durand, S., Melelli, A., Kao, A., Magueresse, A., Dhakal, H., Gorshkova, T., Callebert, F., Bourmaud, A., Beaugrand, J., Guessasma, S., 2021. Novel Insight into the Intricate Shape of Flax Fibre Lumen. Fibers 9. https://doi.org/10.3390/fib9040024.

Richely, E., Nuez, L., Pérez, J., Rivard, C., Baley, C., Bourmaud, A., Guessasma, S., Beaugrand, J., 2022. Influence of defects on the tensile behaviour of flax fibres: cellulose microfibrils evolution by synchrotron X-ray diffraction and finite element modelling. Compos. Part C. Open Access 9, 100300. https://doi.org/10.1016/j.jcomc.2022.100300.

Rwawiire, S., 2016. MECHANICAL AND THERMO-ACOUSTIC CHARACTERIZATION OF BARKCLOTH AND ITS POLYMER REINFORCED COMPOSITES. University of Liberec.

Rwawiire, S., Tomkova, B., 2017. Thermal, static, and dynamic mechanical properties of bark cloth (ficus brachypoda) laminar epoxy composites. Polym. Compos. 38, 199–204. https://doi.org/10.1002/pc.23576.

Rwawiire, S., Tomkova, B., Militky, J., Jabbar, A., Kale, B.M., 2015. Development of a biocomposite based on green epoxy polymer and natural cellulose fabric (bark cloth) for automotive instrument panel applications. Compos. Part B Eng. 81, 149–157. https://doi.org/10.1016/j.compositesb.2015.06.021.

Segal, L., Creely, J.J., Martin, A.E., Conrad, C.M., 1959. An Empirical Method for Estimating the Degree of Crystallinity of Native Cellulose Using the X-Ray Diffractometer. Text. Res. J. 29, 786–794. https://doi.org/10.1177/004051755902901003.

Tamburini, D., Cartwright, C.R., Melchiorre Di Crescenzo, M., Rayner, G., 2019. Scientific characterisation of the dyes, pigments, fibres and wood used in the production of barkcloth from Pacific islands. Archaeol. Anthropol. Sci. 11, 3121–3141. https://doi.org/10.1007/s12520-018-0745-0.

Tanguy, M., Bourmaud, A., Baley, C., 2016. Plant cell walls to reinforce composite materials: Relationship between nanoindentation and tensile modulus. Mater. Lett. 167, 161–164. https://doi.org/10.1016/j.matlet.2015.12.167.

Thibault, J.F., 1979. Automatisation du dosage des substances pectiques par la methode au metahydroxydiphenyle. Leb. Wiss. Technol. 12, 247–251.

Venkatraman, P.D., Scott, K., Liauw, C., 2020. Environmentally friendly and sustainable bark cloth for garment applications: Evaluation of fabric properties and apparel development. Sustain. Mater. Technol. 23, e00136 https://doi.org/10.1016/j.susmat.2019.e00136.

Walusimbi, J.K., 2001. La fabrication des tissus d'écorce en Ouganda [WWW Document]. UNESCO.

Zamil, M.S., Geitmann, A., 2017. The middle lamella—more than a glue. Phys. Biol. 14, 015004 https://doi.org/10.1088/1478-3975/aa5ba5.